

Diamidine Compounds for Selective Inhibition of Protein Arginine Methyltransferase 1

Leilei Yan^{†‡}, Chunli Yan[‡], Kun Qian[†], Hairui Su[§], Stephanie Wofford[‡], Wei-Chao Lee[¶], Xinyang Zhao[§], Meng-Chiao Ho[¶], Ivaylo Ivanov^{‡*}, Yujun George Zheng^{†*}

[†]Department of Pharmaceutical and Biomedical Sciences, College of Pharmacy, The University of Georgia, Athens, Georgia 30602, United States

[‡]Department of Chemistry, Center for Diagnostics and Therapeutics, Georgia State University, Atlanta, Georgia 30302, United States

[§]Stem Cell Institute, Department of Biochemistry and Molecular Genetics, University of Alabama, Birmingham, Alabama 35294, United States

[¶]Institute of Biological Chemistry, Academia Sinica, 128 Sec 2, Academia Road, Nankang, Taipei 115, Taiwan

[‡]Current address: College of Life Sciences, Hebei University. Baoding, Hebei 071002, China

* To whom correspondence should be addressed:

Y. G. Zheng

Tel: (706) 542-0277; Fax: (404) 542-5358; Email: yzheng@uga.edu

I. Ivanov

Tel: (404) 413-5529; Fax: (404) 413-5505; Email: iivanov@gsu.edu

Supporting Information

Compound 1 does not target the substrate of biotin labeled H4-20. The above results suggest that compound **1** is primarily a selective inhibitor for PRMT1 versus the substrate H4-20. To avoid finding inhibitor binding to substrate instead of the enzyme itself and to provide with further evidence that **1** does not target to the substrate peptide, surface plasmon resonance (SPR) assay was performed. Solutions of 80 μM of both **1** and a positive control compound, the PRMT1 inhibitor NS-1 known to target the peptide, were added onto a sensor chip immobilized with biotin labeled H4-20. The result shows that NS-1 interact with the immobilized biotin labeled H4-20 on sensor chip with a K_{on} value of $8.2 \times 10^{-4} \text{ 1}/\mu\text{M}\cdot\text{S}$ and a K_{off} value of $2.1 \times 10^{-3} \text{ 1/S}$ while **1** does not. That means as a PRMT1 inhibitor, **1** does not function by targeting to the substrate peptide of PRMT1 (Figure S-1). Therefore as a primarily competitive inhibitor, **1** can bind and inhibit PRMT1 directly.

The assay was done by using Series S Sensor Chip SA in Biacore™ T200. Biotin labeled H4-20 was dissolved in reaction buffer before being immobilized on a sensor chip. Compound **1** and Compound NS-1, which served as positive control, were dissolved in the same buffer and flowed at a rate of 20 μL pre min for 300 s to allow an association, followed by dissociation over immobilized peptide in reaction buffer.

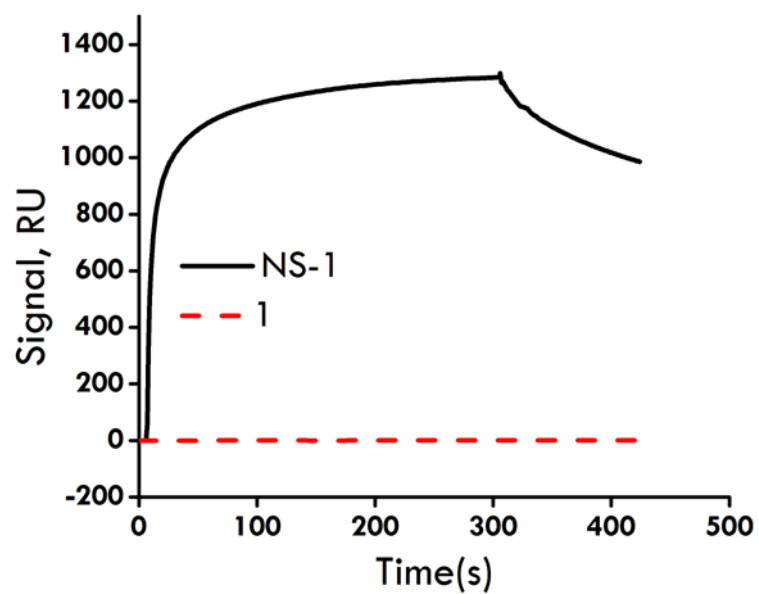


Figure S1. Compound **1** does not interact with biotin labeled H4-20. The positive control compound, NS-1 interacts strongly with biotin labeled H4-20 while **1** doesn't show any interaction with the biotin labeled peptide.

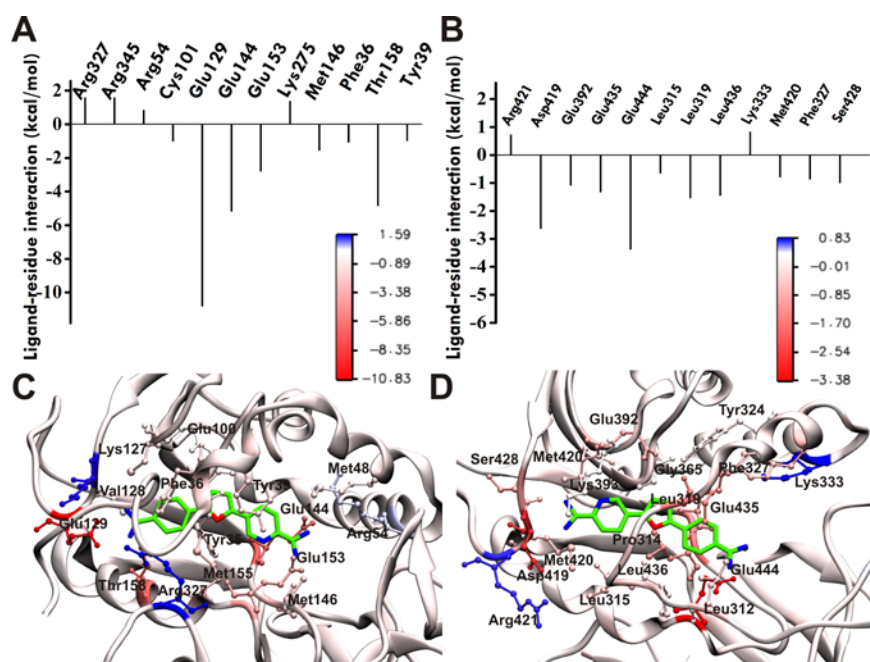


Figure S2. Predicted binding modes of **5** in PRMT1 and PRMT5 from docking (Autodock4.2) and molecular dynamics simulation (NAMD2.8). Ligand-residue interaction energies from MM/PBSA energy decomposition for A) PRMT1 and B) PRMT5. Binding modes of compound **5** with C) PRMT1 and D) PRMT5. The best docking pose obtained from AutoDock for **5** in complex with the hPRMT1 homology model (based on 1F3L¹ and 3SMQ²) and x-ray hPRMT5 (4GQB³) was selected for MD simulation. Dominant structures for the hPRMT1•**5** and hPRMT5•**5** complexes from the last 20ns MD trajectory clustering analysis were used for visualization. PRMT residues engaging the ligand are explicitly shown in ball and stick representation. The protein (in cartoon representation) is colored according to the residue contribution values in the free energy decomposition from red (negative) to blue (positive).

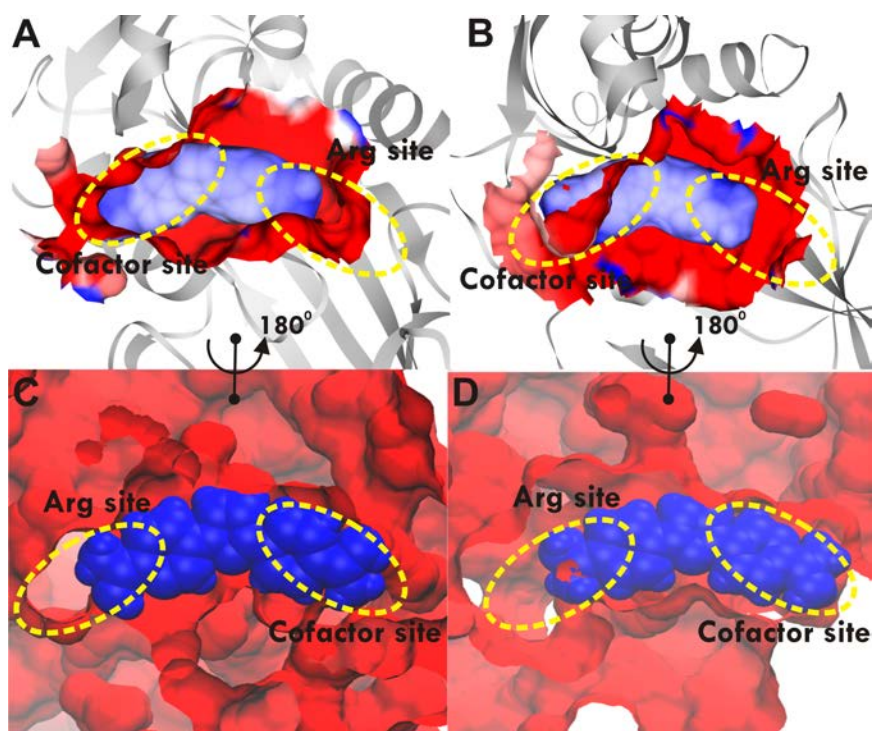


Figure S3. Electrostatic and shape complementarity in diamidine binding to PRTM1 and PRMT5. A) Electrostatic potential surface for the binding pocket of PRMT1 with compound **5**; B) Electrostatic potential surface for the binding pocket of PRMT5 with compound **5**; C) Shape of the binding cavity of PRMT1 (red) with compound **5** (blue); D) Shape of the binding cavity of PRMT5 (red) with compound **5** (blue). The best docking pose obtained from AutoDock for **5** in complex with the hPRMT1 homology model (based on 1F3L¹ and 3SMQ²) and x-ray hPRMT5 (4GQB³) was selected for MD simulation. Dominant structures for the hPRMT1•**5** and hPRMT5•**5** complexes from the last 20ns MD trajectory clustering analysis were used for visualization same as Figure S2 C, D. The charges of proteins were assigned using PDB2PQR server and electrostatic potential was calculated using APBS. The electrostatic potential varied from $-10K_B T/e$ to $+10K_B T/e$ and was depicted using Chimera⁴ in panels A and B from red to blue, respectively. The ligand in panels A and B is color-coded by AM1BCC charge from red (negative) to blue (positive). The surface was visualized in panels C and D using the program VMD.⁵

Table S1. Inhibition of selected compounds on PRMT1 and PRMT5. Screening was carried out by using the filter binding assay with 1 μM H4-20 peptide, 0.5 μM of [^3H]-AdoMet, 0.04 μM of PRMT1 or PRMT5, and 20 μM of a selected diamidine compound.

Diamidine Compounds	Remaining Activity of PRMT1		Remaining Activity of PRMT5	
	Value	Deviation	Value	Deviation
1	0.229	0.026	0.893	0.015
2	0.171	0.022	0.128	0.005
3	0.195	0.066	0.690	0.007
4	0.211	0.067	0.613	0.010
5	0.167	0.047	0.836	0.018
6	0.384	0.068	0.679	0.081
7	0.398	0.160	0.510	0.361
8	0.421	0.103	0.341	0.239
9	0.494	0.082	0.443	0.238
10	0.511	0.124	1.022	0.007
11	0.520	0.100	1.083	0.083
12	0.536	0.107	0.580	0.467
13	0.537	0.138	0.593	0.645
14	0.572	0.024	0.228	0.032
15	0.580	0.178	0.686	0.441
16	0.620	0.137	0.703	0.159
17	0.634	0.166	0.537	0.468
18	0.689	0.053	0.413	0.363
19	0.725	0.266	1.094	0.680
20	0.780	0.009	1.048	0.572
21	0.800	0.090	1.009	0.273
22	0.812	0.092	0.862	0.280
23	0.821	0.033	1.085	0.315
24	0.843	0.182	0.660	0.056
25	0.861	0.234	0.816	0.222
26	0.863	0.122	0.656	0.199
27	0.893	0.011	0.524	0.097
28	0.947	0.185	0.538	0.119
29	0.951	0.093	0.530	0.175
30	0.957	0.212	0.385	0.282

Table S2. Free energy analysis (kcal mol⁻¹) for the binding of ligands to PRMT1 and PRMT5.

Contribution	PRMT1	PRMT5
	5	5
ΔE_{ele}	-560.2(21.3)	-474.9(19.0)
ΔE_{vdw}	-35.7(4.0)	-35.1(2.9)
ΔG_{nonpo}	-5.3(0.1)	-5.9(0.2)
ΔG_{polar}	554.0(16.5)	491.6(16.4)
$\Delta G_{\text{sol}}^{\text{a}}$	548.7(16.5)	485.6(16.4)
$\Delta G_{\text{ele}}^{\text{b}}$	-6.1(11.1)	16.7(8.6)
ΔH_{b}	-47.1(10.0)	-24.3(7.9)
$T\Delta S$	-18.2(8.6)	-18.9(0.6)
ΔG_{b}	-28.9	-6.4
IC_{50} (μM) ^c	9.8	110

^aThe polar/nonpolar ($\Delta G_{\text{sol}} = \Delta G_{\text{polar}} + \Delta G_{\text{nonpolar}}$) contributions. ^bThe electrostatic ($\Delta G_{\text{ele}} = \Delta E_{\text{ele}} + \Delta G_{\text{polar}}$) contributions. ^c IC_{50} for rat PRMT. Standard deviation values are shown in parentheses.

References:

1. Zhang, X.; Zhou, L.; Cheng, X. Crystal structure of the conserved core of protein arginine methyltransferase PRMT3. *EMBO J.* **2000**, *19*, 3509-3519.
2. Siarheyeva, A.; Senisterra, G.; Allali-Hassani, A.; Dong, A.; Dobrovetsky, E.; Wasney, G. A.; Chau, I.; Marcellus, R.; Hajian, T.; Liu, F.; Korboukh, I.; Smil, D.; Bolshan, Y.; Min, J.; Wu, H.; Zeng, H.; Loppnau, P.; Poda, G.; Griffin, C.; Aman, A.; Brown, P. J.; Jin, J.; Al-Awar, R.; Arrowsmith, C. H.; Schapira, M.; Vedadi, M. An allosteric inhibitor of protein arginine methyltransferase 3. *Structure* **2012**, *20*, 1425-1435.
3. Antonysamy, S.; Bonday, Z.; Campbell, R. M.; Doyle, B.; Druzina, Z.; Gheyi, T.; Han, B.; Jungheim, L. N.; Qian, Y.; Rauch, C. Crystal structure of the human PRMT5: MEP50 complex. *Proc. Natl. Acad. Sci. USA.* **2012**, *109*, 17960-17965.
4. Pettersen, E. F.; Goddard, T. D.; Huang, C. C.; Couch, G. S.; Greenblatt, D. M.; Meng, E. C.; Ferrin, T. E. UCSF Chimera—a visualization system for exploratory research and analysis. *J. Comput. Chem.* **2004**, *25*, 1605-1612.
5. Humphrey, W.; Dalke, A.; Schulten, K. VMD: visual molecular dynamics. *J. Mol. Graphics* **1996**, *14*, 33-38.